

Electronic energy bands in the fluorite structure: CaF_2 and CdF_2

J. P. Albert, C. Jouanin, and C. Gout

Centre d'Etudes d'Electronique des Solides, associé au Centre National de la Recherche Scientifique, Université des Sciences et Techniques du Languedoc, Place E. Bataillon, 34060 Montpellier Cedex, France

(Received 25 July 1977)

The electronic band structures of calcium and cadmium fluoride are calculated by a combined tight-binding and pseudopotential method. The overall shape of the valence bands is found to be the same in these two compounds and agrees quite well with a "universal valence-band structure" calculated for the fluorite structure. Yet it is found that the excited cationic d states lie too high in the conduction band. It is then shown that with a simple semiempirical modification of the cationic pseudopotential model a coherent interpretation of the optical spectra of the two crystals can be proposed.

I. INTRODUCTION

The present paper is concerned with the calculation of the electronic band structure of two fluoride compounds having the "fluorite" structure, e.g., calcium and cadmium fluoride. Both are highly ionic, wide-gap insulators which have been subjected to numerous investigations devoted to their intrinsic optical properties in relation with their band structure. Optical measurements on CaF_2 in the vacuum-ultraviolet region have been carried out by Tomiki¹ *et al.* near the absorption edge, Stephan *et al.*,² Rubloff,³ and Hayes *et al.*⁴ for photon energies up to 40 eV, Le Comte *et al.*⁵ up to 70 eV. Frandon⁶ and Lahaye⁷ have measured characteristic energy losses up to 140 eV and their results are in good agreement with these optical spectra. Ultraviolet and x-ray photoelectron studies (UPS and XPS) have also been reported by Poole *et al.*⁸ and Bremser⁹ who succeeded in determining the position and width of the upper occupied bands.

Cadmium fluoride has also received much attention owing to its unusual properties when doped. Reflectivity measurements have been reported by Forman¹⁰ *et al.* and Eisenberger *et al.*¹¹ near the fundamental optical gap and by Berger¹² *et al.* and Bourdillon¹³ *et al.* up to 60 eV.

However, despite the availability of this extensive experimental data, the interpretation of the spectra has been found rather difficult due to the lack of theoretical work on the fluorite structure. In fact, except for the work of Starostin *et al.*^{14,15} and Ganin *et al.*,¹⁶ the discussions and interpretations of the great majority of the available measurements lay on empirical band schemes^{1,2,7,17} which are highly incomplete and are found to disagree somewhat with each other. All these facts make the ordering of levels uncertain, particularly the location of the bottom of the conduction band.

It is expected that in CaF_2 the lower conduction

bands originate from mixing of the unoccupied $4s$ and $3d$ Ca^{++} states, as is the case in CaO . This fact has been found to produce in this crystal secondary¹⁸ and even absolute minima at the X point,^{19,20} according to the various calculations. On these grounds, Tomiki¹ *et al.* and Frandon⁶ and Lahaye⁷ based their interpretation on the occurrence of the minimum of the conduction band at the X point, while Rubloff³ deduced the conduction bands of CaF_2 from that of KCl and hence postulated the absolute minimum to lie at the Γ point with the possibility of a secondary minimum at X .

In CdF_2 , the cationic unoccupied $5d^+$ states are expected to lie somewhat higher in energy and certainly do not perturb significantly the bottom of the conduction bands, which originates chiefly from the $6s$ Cd^{++} levels, as it has been found to be the case in CdO .²¹⁻²³ Yet, despite these facts, the occurrence of the minimum of the conduction band at Γ , as is the case for an s -like band, is not fully accepted. For example, Lee and Moser²⁴ obtained a consistent picture of the optical and transport properties of donors in CdF_2 , when assuming the conduction band to be multivalleyed with a minimum at X .

Concerning the occupied bands of these two fluorides compounds, a simple electrostatic model predicts that the upper valence bands are principally formed by the p F^- orbitals. However, the cationic $4d$ Cd^{++} states are expected to lie close below them in CdF_2 ; this p - d mixing can thus affect strongly these upper levels and produce valence-band maxima away from Γ , as has been shown to occur in CdO ,²¹⁻²³ and the silver halides.²⁵ Despite these possible differences between the band structure of these two crystals, the comparison of their reflectivity spectra shows a striking resemblance in shape for the low-energy peaks lying on the high-energy side of the absorption edge. Although widely noticed^{12,13} this similarity has not

yet received a satisfactory explanation and it has even been postulated that this fact was accidental.¹³

It appeared thus interesting to calculate the energy bands of both CaF₂ and CdF₂ using the same method and the same approximations in order to get further insight into the behavior of the electronic energy levels in the fluorite structure and into the possible influence of the cation on these bands. The choice of these two materials seems particularly well suited to this study because not only do CaF₂ and CdF₂ crystallize in the same structure, but their lattice constants are very similar (10.32 a.u. for CaF₂, 10.18 a.u. for CdF₂). The eventual differences that arise in their band structures can thus undoubtedly be attributed to the different electronic structure of the cations.

Recently, we performed a band-structure calculation of CaF₂ with a mixed linear-combination-of-atomic-orbitals (LCAO)-orthogonalized-plane-wave (OPW) method.²⁶ In that work, first we calculated explicitly all three center terms arising in the tight-binding part of the calculation and then we orthogonalized the empty levels to the previously determined occupied states. The energy bands obtained were found to give a fairly satisfactory explanation of some of the existing features in the optical spectra. However, as is common with the OPW method, the *d*-like conduction bands were found to be poorly converged and thus appeared to lie too high in the band scheme. As the application of this method to CdF₂ appeared to be too cumbersome and in order to be able to correct easily this drawback of the OPW method, we decided to use in this work a simplified version of that calculation using a "spherical version" of the LCAO calculation and a model pseudopotential for the calculation of the empty bands.²⁷ In Sec. II we describe our method of calculation and obtain the energy-band structure of CaF₂ and CdF₂. In Sec. III we compare these bands with each other and with the experimental data. Yet it is shown that in our standard pseudopotential method as well as in our previous OPW study the excited *d* states lie too high in the conduction-band scheme. A semiempirical correction is then introduced which allows a coherent interpretation of both CaF₂ and CdF₂ experimental data. The most important results of our study are resumed in Sec. IV.

II. CALCULATION AND RESULTS

We shall give here a brief outline of the methods we have used, stressing only the essential features and approximations of our calculation. More details will be found in Refs. 28 and 29, where the same methods were used.

A. Valence and core bands

The method used for these states is the tight-binding method with a "spherical" approximation version for the calculation of three center terms.

(i) The Bloch sums were constructed on the 2*s*, 2*p* F⁻ states together with the 3*p* Ca⁺⁺ orbitals in the case of CaF₂ and 4*d* Cd⁺⁺ states for CdF₂. (The other core states have been verified to produce negligible contributions to the higher bands). The ionic wave functions were those calculated analytically by Richardson³⁰ for Cd⁺⁺ and Salez³¹ for Ca⁺⁺ and F⁻ by the Hartree-Fock method.

(ii) The potential has been decomposed as usual into its Coulombic and exchange contributions.

(iii) The Coulombic part of the crystal potential has been taken as the superposition of the individual free ion potentials as is commonly done in dealing with ionic crystals.

(iv) For the exchange part, we used the Slater $\rho^{1/3}$ approximation.³² In order to suppress the well-known unphysical low-density tail of this approximation, we have adopted a muffin-tin version of this term, calculating it inside spheres with half nearest-neighbor radius centered at each ion site and annulling it in the small-charge-density regions between these spheres.²⁶

In order to calculate the matrix elements of the Hamiltonian between atomic orbitals u_μ and $u_{\mu'}$ centered at \vec{d}_i and \vec{d}_j , we made the following "spherical" approximation:

$$\begin{aligned} \langle u_\mu(\vec{r} - \vec{d}_i) | H | u_{\mu'}(\vec{r} - \vec{d}_j) \rangle \\ = \frac{1}{2}(\epsilon_\mu + \epsilon_{\mu'}) S_{\mu i, \mu' j} + \frac{1}{2} [\langle u_\mu(\vec{r} - \vec{d}_i) | U_j^s | u_{\mu'}(\vec{r} - \vec{d}_j) \rangle \\ + \langle u_\mu(\vec{r} - \vec{d}_i) | U_i^s | u_{\mu'}(\vec{r} - \vec{d}_j) \rangle]. \end{aligned} \quad (1)$$

$U_{i(j)}^s$ is the spherical average calculated around site *i* (*j*) of the sum over the lattice of the individual ionic potential minus that of ion *i* (*j*). $S_{\mu i, \mu' j}$ is the overlap matrix element and $\epsilon_{\mu(\mu')}$ is the ionic energy of the orbital $u_{\mu(\mu')}$. In order to obtain a good convergence of the energy bands, we had to include contributions up to the third neighbor in the calculation of the interaction between the F⁻ ions.

The results for the occupied bands of CaF₂ and CdF₂ are shown in Figs. 1 and 2, respectively. The energy of these levels at high-symmetry Γ , X, L points are given in Table I. For the two crystals the lowest bands originate from the 2*s* F⁻ levels. These are practically flat and situated at nearly the same energy (≈ -2.9 Ry in the two cases). This is due to the low extension of these 2*s* F⁻ wave functions which do not mix appreciably with the upper ones and are simply displaced in the crystal by the Madelung energy which is near-

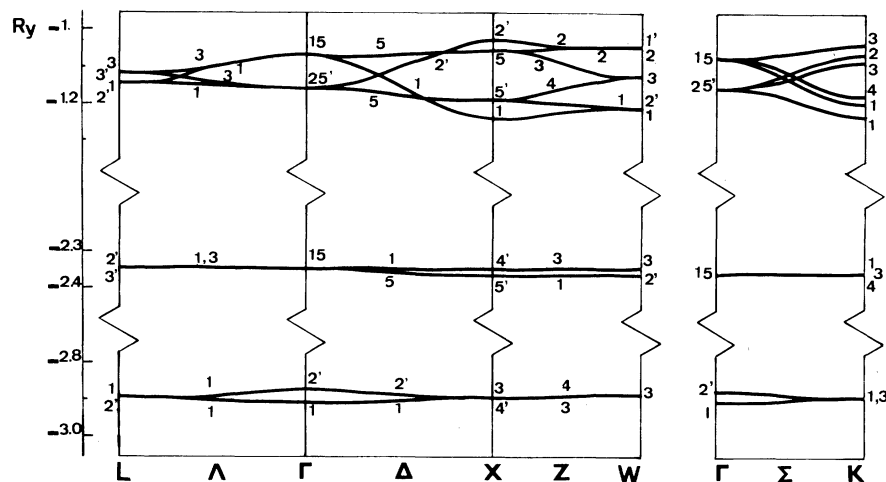


FIG. 1. Valence and core bands of CaF_2 (tight-binding method).

ly the same for CaF_2 and CdF_2 . We then find in CaF_2 at about -2.35 Ry the bands proceeding from the $3p$ Ca^{++} states, while the $4d$ Cd^{++} states are situated higher, at -1.32 Ry, in CdF_2 . These bands are both very narrow and their positions agree well with what can be expected from a simple electrostatic model.

The upper valence bands in the two crystals originate mainly from the p F^- orbitals with a slight admixture of $4d$ Cd^{++} states in CdF_2 . These bands are quite similar in shape, that of CdF_2 being wider (3.5 eV) than that of CaF_2 (2.7 eV). This is due to the smaller distance between the anion sites in CdF_2 than in CaF_2 . The striking similarity of these bands, despite the closeness of the d^+ cationic states in CdF_2 , shows clearly that these states have only a negligible effect on the overall shape of the anion levels in the fluorite structure. This can also be verified in decoupling the d^+ and p^- states in the CdF_2 calculation. Although the energy

levels with the same symmetry are modified, the whole shape of these upper bands as well as their ordering remains the same. This results from the fact that, in the fluorite structure, a mixing between d^+ and p^- states occurs at Γ and thus the hybridization between them does not affect much the shape of the bands along the axes, contrary to what happens in CdO which crystallizes in the rock-salt structure.²¹⁻²³

B. Conduction bands

For the calculation of the empty bands, we have adopted the pseudopotential method developed by Bassani³³ and Giuliano³⁴ and modified by us²⁸ in the calculation of the energy bands in alkali fluorides. In that method, the conduction states are calculated as those of an extra electron added to the lattice. The orthogonalization to the lower occupied energy states is taken into account by the use of a model pseudopotential which, in highly ionic solids like

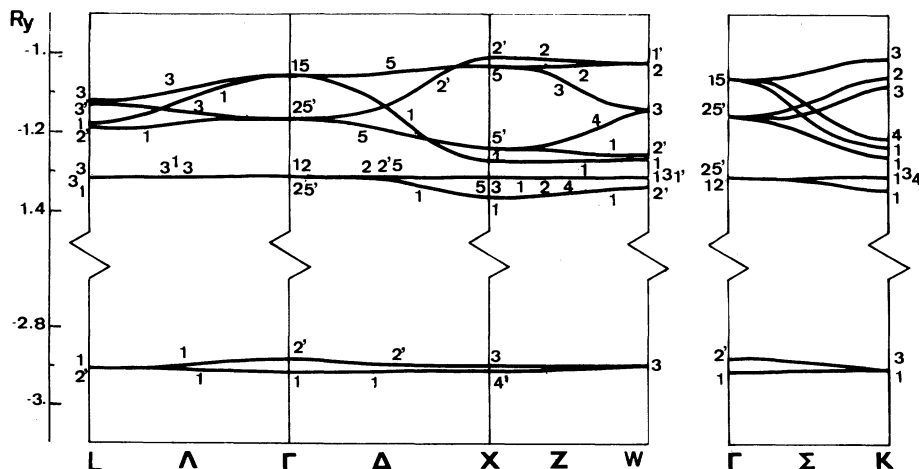


FIG. 2. Valence and core bands of CdF_2 (tight-binding method). Some d bands have been sketched on the same line because of their closeness.

TABLE I. Valence and core-band energies of CaF_2 and CdF_2 at Γ , X , and L points (in Ry).

Levels	CaF_2	CdF_2
Γ_1	-2.896	-2.917
Γ'_2	-2.875	-2.885
Γ_{15}	-2.343 -1.065	-1.059
Γ'_{25}	-1.148	-1.321 -1.161
Γ_{12}		-1.313
X_1	-1.233	-1.359 -1.267
X'_4	-2.889 -2.336	-2.908
X'_2	-1.032	-1.008
X_2		-1.311
X_3	-2.882	-2.900 -1.315
X'_5	-2.350 -1.185	-1.242
X_5	-1.047	-1.310 -1.030
L_1	-2.886 -1.142	-2.904 -1.316 -1.178
L'_2	-2.342 -2.886 -1.142	-2.901 -1.182
L_3	-1.116	-1.320 -1.311 -1.119
L'_3	-2.346 -1.114	-1.133

these ones, can be obtained as the superposition of the individual ionic ones. For the positive ions, the pseudopotential is constructed according to the Philipps and Kleinman³⁵ approach:

$$V_{ps}^+ = V_a + \sum_c (E - E_c) |c\rangle \langle c|. \quad (2)$$

V_a is the bare ionic potential and the sum extends over the occupied cationic states $|c\rangle$, E_c being their energy in the crystal. For the F^- ions, the analytic form of Bassani and Giuliano is used:

$$V_{ps}^- = \sum_l V_l P_l, \quad (3)$$

where

$$V_l(r) = -\frac{e^2 N e^{-\alpha_l r}}{r} - \frac{Z e^2}{r + A_l / r^2}. \quad (4)$$

TABLE II. F^- parameters of the pseudopotential.

α_s	α_p	α_d	A_s	A_p	A_d
90	90	2.5	0.75	0.5	2

P_l is the angular momentum projection operator, Z and N are the valence and nuclear charges, and the parameters α_l and A_l are angular momentum dependent. The values of these F^- parameters are those already determined by us in the calculation of the band structure of the alkali fluorides²⁸ and are listed in Table II. It is to be noted that this same approach has been found particularly efficient and has given useful information in its application to alkali fluorides,²⁸ magnesium fluoride,²⁹ and some oxides.^{18,36} Further comment on the choice of the parameters and on the details of the calculation will be found in these papers and in Ref. 33.

In Fig. 3 and 4 we have plotted the calculated conduction bands of CaF_2 and CdF_2 . The energies of Γ , X , and L states are given in Table III. As can be seen from these schemes the behavior of the bands are similar for the two fluorides, the s state Γ_1 being the absolute minimum in the two cases. However, the d -like states are seen to lie higher in CdF_2 than in CaF_2 because of the repulsion of the occupied $3d^+$ and chiefly $4d^+$

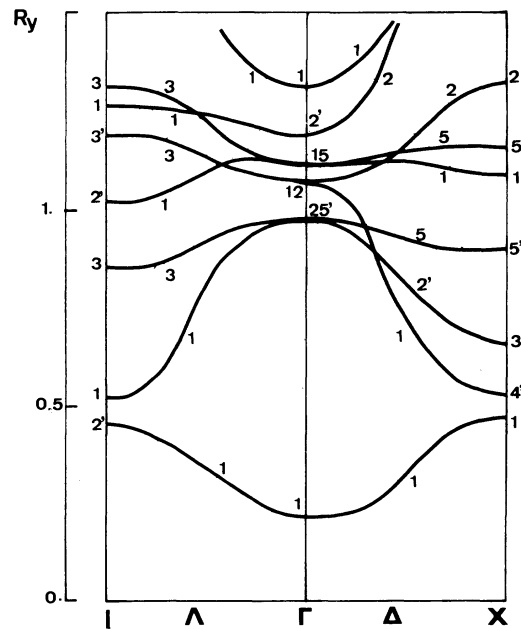
FIG. 3. Conduction bands of CaF_2 (pseudopotential method).

TABLE III. Conduction-band energies of CaF_2 and CdF_2 at Γ , X , and L points (in Ry).

Levels	CaF_2	CdF_2
Γ_1	0.224	0.041
	1.315	1.238
Γ'_{25}	0.990	1.089
Γ'_2	1.189	1.204
Γ_{12}	1.085	1.186
Γ_{15}	1.130	0.958
	1.657	1.492
X_1	0.479	0.421
	1.103	0.726
	1.686	1.776
X_3	0.672	0.741
X'_4	0.530	0.345
X_5	1.166	1.140
X'_5	0.919	0.732
X_2	1.325	1.450
L_1	0.522	0.356
	1.266	1.094
L_3	0.852	0.930
	1.314	1.424
L'_2	0.467	0.327
	1.026	1.008
L'_3	1.196	0.940

states, and so they are decoupled from the lower s -like states.

III. DISCUSSION OF RESULTS

A. Occupied bands

Besides our previous work on CaF_2 ,²⁶ Starostin has calculated the fluorite energy bands; he calculated first the valence and core bands with a tight-binding method,¹⁴ neglecting all three center terms, and then he obtained the whole band structure using the OPW method.¹⁵ All the band struc-

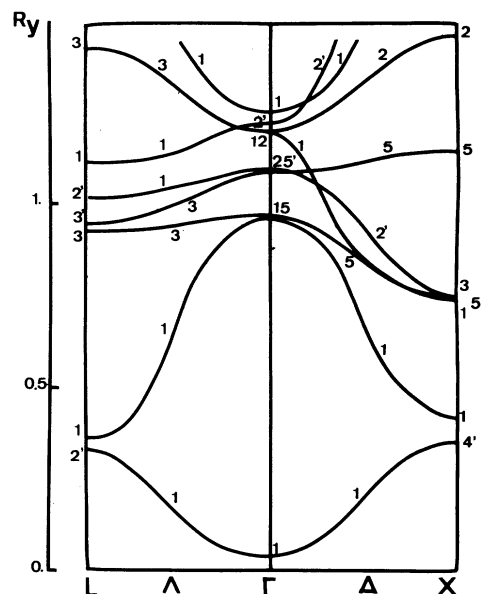


FIG. 4. Conduction bands of CdF_2 (pseudopotential method).

tures obtained in these works are in good qualitative agreement with the scheme given here; chiefly the occupied bands whose shape and sequence of levels are quite similar.

In particular, in all the calculations, the maximum width of the valence band lies at the X point and results from the energy difference between the bonding (X_1) and antibonding (X'_2) combinations of p^- levels. In Table IV we report theoretical as well as experimental results concerning the energy separation of the valence and core bands in CaF_2 . As can be seen, the agreement between our two calculations is quite good and our results compare favorably with photoemission data.

Yet the widths of the valence bands are very sensitive to the methods and approximations used. Starostin finds a width of 3.2 eV with the OPW method, 8.97 eV with his tight-binding method, and we find 1.6 and 2.7 eV according to the approximations we made in the calculation of the potential-energy matrix elements. The unrealistic 8.97-eV

TABLE IV. Comparison between theoretical and experimental results for the relative positions and widths of the valence and core bands in CaF_2 . Energies are in eV. The zero of energy is taken at the center of the valence band.

	Starostin <i>et al.</i> (Refs. 14 and 15)	Hayes <i>et al.</i> (Ref. 4)	Albert <i>et al.</i> (Ref. 26)	This work	Bremser (Ref. 9)	Poole <i>et al.</i> (Ref. 8)
Ca^{++} ($3p$)	19.1		16.9	16.8	17.1	17.3
F^- ($2s$)	24.3	24.3	20.1	24	21.4	22
Valence-band width	8.97 3.2		1.6	2.7	1.2	3.0 (HW) 4.8 (TW)

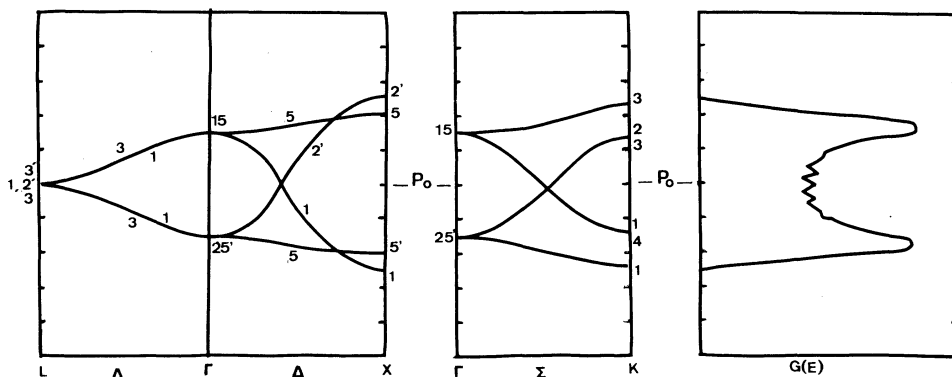


FIG. 5. Universal valence-band structure and density of states of fluorite-type compounds in units of V_{σ} . p_0 is the energy of the atomic anion p level in the crystal and $G(E)$ is the density of states.

value found by Starostin¹⁴ is surely due to the neglect of all the three center terms in his calculation; this also affects the relative positions of the occupied band. The difference between our two calculations results surely from our spherical approximation which overestimates the potential and thus the Hamiltonian matrix elements. However, as is usually the case, the calculated bandwidths using Slater's exchange are smaller than those deduced from photoemission data. Poole *et al.* report 4.8 and 3 eV, respectively, for the total width (TW) and full width at half maximum (FWHM) of the peak corresponding to the valence band.

Concerning CdF_2 , our calculation seems to be the only existing one and, to our knowledge, no XPS or UPS data have been reported for this material. As has been already said, the upper valence bands of CdF_2 are quite similar to those of CaF_2 and are not much distorted by the cationic d^+ levels. The width of those d^+ bands is found to be about 0.7 eV in our calculation; this value can be compared with that found in CdO calculations by Tewari²¹ and Maschke²² *et al.* (about 1.3 eV). This difference is here also explained by the smaller distance between the cation sites in CdO than in CdF_2 .

An interesting feature common to all the band structure calculations in the fluorite structure is the marked tendency of X'_2 and in some cases X'_5 to lie above Γ_{15} . This behavior seems thus characteristic of the p anion bands in this structure.

In order to get a further evidence of this fact, we have calculated an "universal valence-band scheme" for the p^- levels, along the lines suggested by Pantelides³⁷ in his study of the rocksalt structure. Pantelides' study has proven adequate and useful in describing and predicting the behavior of anion levels in this structure and so we have extended his ideas to the fluorite structure. The band-structure calculation is essentially based on the tight-binding two-center approximation, with

only one parameter, namely the σ interaction between the nearest-neighbor p anion states. Details of the calculation can be found in the Appendix and in Pantelides' paper. The resulting energy bands together with the corresponding density of states are sketched in Fig. 5. These bands are seen to be in quite good qualitative agreement with those found by more sophisticated methods. In particular, they possess the same features as those we found for CaF_2 and CdF_2 , the only slight deviations being due to the neglect of three center terms and of the interactions between more distant neighbors. Indeed, an interesting fact which arises from this study is the presence of the maximum of the upper valence band at X point instead of Γ , as is the case with p bands in the rocksalt structure. The bands and the corresponding density of states are shown to be symmetrical with respect to the middle of $\Gamma'_{25} - \Gamma_{15}$, this symmetry being only destroyed by the introduction of the interaction between the anion p levels and the cationic core p^+ or d^+ states.

B. Conduction bands

We report in Figs. 6 and 7 the reflectivity data obtained by Rubloff³ on CaF_2 and by Bourdillon¹³ *et al.* on CdF_2 (as noted by these authors the lower-energy part of this spectrum up to 8.5 eV is taken from Eisenberger¹¹). The other experimental works carried out on these crystals are essentially in good agreement with these within their relative energy range.

The comparison between these two spectra shows clearly that the shape of the low-energy peaks extending from the edge up to 17 eV is quite similar in the two crystals. The first peak, occurring at 11.18 eV in CaF_2 and 7.6 eV in CdF_2 has been attributed to the direct band-gap exciton. The workers^{3,11} who obtained these spectra deduced a band gap of 12.1 eV for CaF_2 and 9.4 eV for CdF_2 .

At this point, it is to be noted that the comparison between a theoretical one-electron energy-band

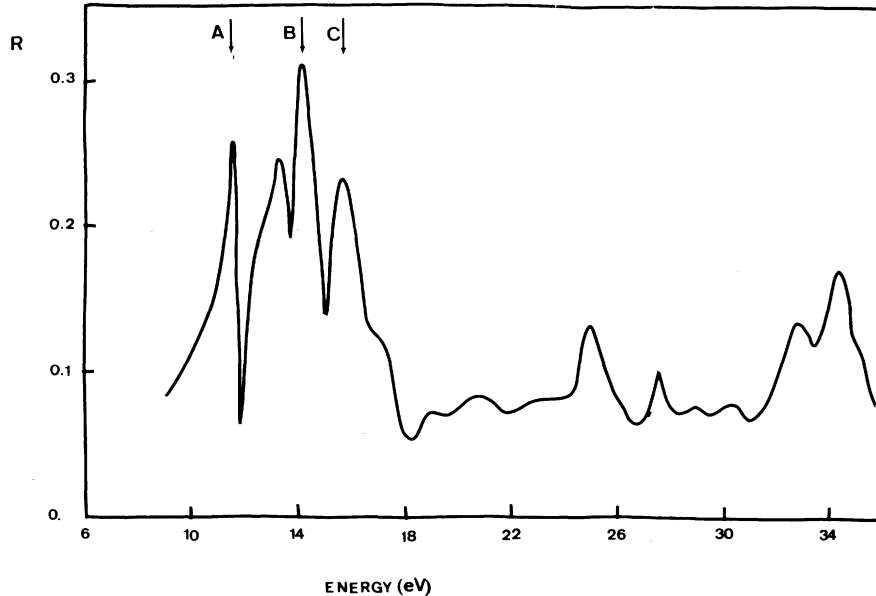


FIG. 6. Reflectance spectrum of CaF_2 at room temperature (after Rubloff, Ref. 3).

structure and the experimental optical data must include the correlations effects. These have been discussed at length by Fowler,³⁸ Perrot *et al.*,³⁹ and Pantelides⁴⁰ *et al.* who have shown that, when considering transitions of an electron from an occupied band to an empty one, a polarization correction must be taken into account. As has been observed by these authors, the main effect of these polarization corrections is to shift about rigidly the bands without large change in their shape. Thus, our theoretical band gap must be reduced by this correction before comparing our results with the optical spectra. Fowler³⁸ has evaluated this polarization correction for insulators with fcc structure using the Mott-Littleton⁴¹ approximation. Unfortunately this correction has not been calculated for CaF_2 and CdF_2 . In fact, because of the rather approximate treatment of this term we have decided not to calculate it and to simply shift the bands rigidly in order to match the experimental optical gap before comparing our results with the reflectivity spectra. This amounts to reducing the theoretical band gap by 0.40 Ry in CaF_2 and 0.41 Ry in CdF_2 . These values are in fact in good agreement with those already calculated by Fowler and used by us in our study of the alkali fluorides²⁸ and magnesium fluoride²⁹: 0.25 Ry for KF, 0.265 Ry for NaF, 0.35 Ry for LiF, and 0.45 Ry for MgF_2 . We have then to consider the following experimental peaks which extend up to 17 eV. Within this energy range the experimental features are quite similar in shape for the two materials and are to be associated with transitions from the upper valence bands. However, there is

some difficulty in explaining these peaks with our calculated condition-band schemes. This is due to the too high position of the cationic *d*-like levels in our calculations. The problem arising here is of the same nature as that we have already met in our previous OPW calculation on CaF_2 ,²⁶ namely the inadequacy of the OPW or pseudopotential method in their standard form when dealing with *d* bands. That seems also to be the case in the band-structure calculation of Vasvari⁴² *et al.* in alkaline-earth metals. The Heine-Abarenkov potential they employed situates the empty *d* levels far higher than the augmented-plane-wave (APW)⁴³ or Korringa-Kohn-Rostoker (KKR)⁴⁴ methods. The same is true for the calculation of Daude *et al.* on

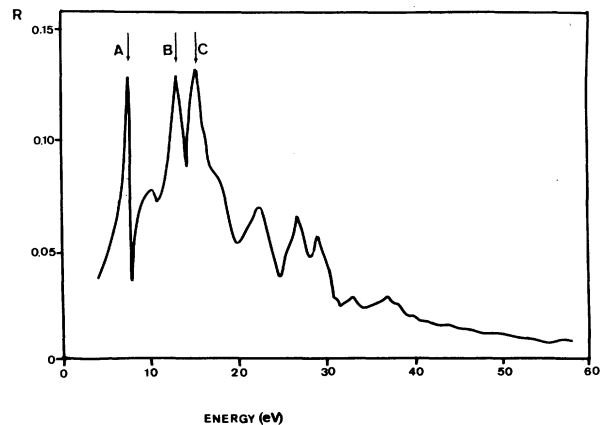


FIG. 7. Reflectance spectrum of CdF_2 at room temperature (after Bourdillon, Ref. 13).

CaO¹⁸ with the same pseudopotential model as that used here. They find the cationic d state X_3 to be secondary minimum in the conduction band, whereas Seth¹⁹ and Mattheiss²⁰ using LCAO and APW methods, respectively, find it to be the absolute minimum, slightly below Γ_1 . Further evidence for the incorrect position of these d states in our scheme can be gained by considering the strong broad doublet extending in the CaF₂ spectrum from 31 to 35 eV. This same doublet is found in calcium compounds such as CaF₂, CaCl₂, CaI₂,⁵ and CaO,⁴⁵ and is thus characteristic of the Ca⁺⁺ ion. However, the $p-d$ Ca⁺⁺ transitions $\Gamma_{15}(p^*) \rightarrow \Gamma'_{25}(d^*)$, $\Gamma_{15}(p^*) \rightarrow \Gamma_{12}(d^*)$, $X'_5(p^*) \rightarrow X_3(d^*)$ are evaluated in our scheme at 41, 39.9, and 35.6 eV, respectively, higher than the experimental data. Several ways of improving of the OPW and pseudopotential method have been proposed.⁴⁶ We have adopted here the procedure developed by Fong and Cohen⁴⁷ and Animalu⁴⁸ (in a quite similar form) in their treatment of d bands in transition metals and KCl.⁴⁹ In this method, one simply adds a partial d wave potential well to the standard potential. Thus in our case the cationic effective pseudopotential becomes

$$U_{ps}^* = V_{ps}^* + U_2 P_2. \quad (5)$$

V_{ps}^* is the standard pseudopotential Eq. (2), P_2 the $l=2$ projection operator, and U_2 is the depth of the well.

$$U_2(r) = \begin{cases} A, & r < R_M \\ 0, & r > R_M. \end{cases} \quad (6)$$

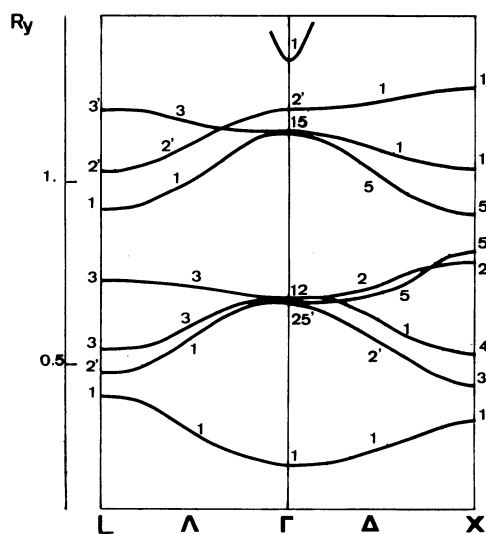


FIG. 8. Corrected conduction bands of CaF₂ (modified pseudopotential method).

TABLE V. Energies of the d -like states in the corrected conduction bands of CaF₂ and CdF₂ (in Ry).

Levels	CaF ₂	CdF ₂
Γ'_{25}	0.665	0.727
Γ_{12}	0.681	0.735
X_1	0.346	0.339
	1.034	0.629
	1.251	1.192
X_2	0.776	0.816
X_3	0.440	0.492
X_5	0.802	0.820
L_1	0.407	0.320
	0.926	0.713
L_3	0.539	0.582
	0.730	0.741

The radius R_M of that well has been taken as half the nearest-neighbor distance. The parameter A has been determined in the following way.

We have performed a conduction-band calculation of CaO with this model pseudopotential Eq. (5) for Ca⁺⁺ and the anion model potential used by Daude *et al.* for O²⁻.¹⁸ The constant A has then been adjusted in such a way that we obtained a band scheme in accord with that found by Seth¹⁹ and Mattheiss²⁰ (e.g., until we obtained the d X_3 level slightly below Γ_1). This was the case for $A = -1.2$ Ry. The same model Ca⁺⁺ potential has then been used to calculate the conduction band of CaF₂. The resulting bands are plotted in Fig. 8. In Table V we give the resulting energies of the Γ , X , and L levels affected by this correction, e.g., those of d symmetry states. (The energies of the other states remains evidently unchanged and can be obtained from Table III.) As it can be seen on Fig. 8 the d -like conduction levels lie now lower with respect to the lowest conduction states than in the preceding pseudopotential and OPW calculations.²⁶ Nevertheless, the pure d -like X_3 state which was the absolute minimum of the conduction band in CaO is now a relative minimum and lies even above X_1 in CaF₂. This is due to the existence in the fluorite structure of a linear combination of occupied anion s levels with this same X_3 symmetry which repels upward the empty level. That seems to rule out definitively the possibility for the minimum of the conduction band of CaF₂ to be X_3 as it was postulated by some authors.^{1,6,7} We are now in position to compare our results with experimental reflectivity data on CaF₂.

1. Comparison with CaF_2 optical spectra

The sharp structure and the temperature dependence of the peaks situated at 13.9 and 15.5 eV in the Rubloff spectrum suggests strongly that they are due to excitons presumably associated with the d conduction bands. In our band scheme X_3 is found to be a relative conduction-band minimum and these peaks may thus be attributed to resonant excitons associated with the allowed $X_2' - X_3$, $X_5' - X_3$ transitions. These transitions are evaluated at 14.6 and 16.6 eV, respectively. When taking into account a binding energy for the valence excitons of the order of 1 eV, as is usually the case for ionic solids, these assignments do not seem to be too unreasonable. In our previous OPW study the following large peak at 25 eV has been attributed to the transition $\Gamma_{25}'(p^-) - \Gamma_{15}$.

The present study situates the same transition at 25.5 eV in good agreement with our previous result (24 eV)²⁶ and the experimental value. The sharp peak at 27.7 eV has been identified as the core $\Gamma_{15}(p^+) - \Gamma_1$ exciton.^{3,26} The corresponding interband transition is found at 29.4 eV in good agreement with our previous calculation (29.6 eV). The binding energy deduced for this core exciton is also in very good agreement with that calculated by Hönerlage *et al.*⁵⁰ (1.68 eV). We then find the broad doublet at 32.8 and 34.5 eV. These structures are known to be transitions characteristic of the Ca^{++} ion.⁵¹ Contrary to what was found in our OPW and standard pseudopotential approach the theoretical transition energies $X_5(p^+) - X_3(d^*)$

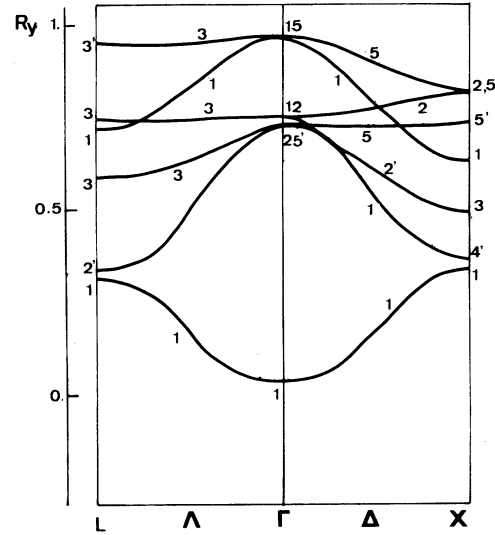


FIG. 9. Corrected conduction bands of CdF_2 (modified pseudopotential method).

(32.5 eV) and $\Gamma_{15}(p^+) - \Gamma_{25}'(d^*)$, $\Gamma_{15}(p^+) - \Gamma_{12}(d^*)$ (35.5 eV) are now in accord with the experimental data. Transitions from 2s F^- levels begin at about 38 eV in our scheme and can thus explain the weak structures on the high-energy side of this doublet.

2. Comparison with CdF_2 optical spectrum

Concerning CdF_2 , we have used as a guideline in our tentative interpretation the great similarity

TABLE VI. Tentative interpretation of the optical spectra of CaF_2 and CdF_2 . Energies are in eV.

Reflectivity CaF_2 (Ref. 3)	Interpretation	Theoretical value	Reflectivity CdF_2 (Ref. 12)	Interpretation	Theoretical value
11.2	$\Gamma_{15} \rightarrow \Gamma_1$ exciton	Transition at 12.1	7.6	$\Gamma_{15} \rightarrow \Gamma_1$ exciton	Transition at 9.4
13.9	$X_2' \rightarrow X_3$ exciton	Transition at 14.6	13.1	$X_2' \rightarrow X_3$ exciton	Transition at 14.8
15.5	$X_5' \rightarrow X_3$ exciton	Transition at 16.6	15.2	$X_5' \rightarrow X_3$ exciton	Transition at 18
25.1	$\Gamma_{25}'(p^-) \rightarrow \Gamma_{15}$	25.5	23.1	$\Gamma_{25}'(p^-) \rightarrow \Gamma_{15}$	23.2
	Core exciton	Transition at 29.5	27.1	$\Gamma_{12}(d^+) \rightarrow \Gamma_{15}$	
27.7	$\Gamma_{15}(p^+) \rightarrow \Gamma_1$		29.7	$\Gamma_{25}'(d^+) \rightarrow \Gamma_{15}$	25.3
32.8	$X_5'(p^+) \rightarrow X_3$	32.5			
34.75	$\Gamma_{15}(p^+) \rightarrow \Gamma_{25}', \Gamma_{12}$	35.5, 35.7			
≈ 37	$\left\{ \begin{array}{l} X_4'(s^-) \rightarrow X_1 \\ L_1(s^-) \rightarrow L_2' \\ L_2'(s^-) \rightarrow L_1 \end{array} \right.$	38.6	37.7	$\left\{ \begin{array}{l} X_4'(s^+) \rightarrow X_1 \\ L_1(s^-) \rightarrow L_2' \\ L_2'(s^-) \rightarrow L_1 \end{array} \right.$	38.6
		40.2			38.2
≈ 39		39.2			38.3
			43	$X_3(s^-) \rightarrow X_5'$	43.8

between the peaks extending from the edge up to 17 eV in the optical spectra of CaF_2 and CdF_2 . This experimental feature and the fact that the upper valence bands are quite similar in the two crystals suggest strongly that the same assignment can be made for the peaks labeled A, B, and C in the two spectra (Figs. 6 and 7). Peak A is then assigned to the $\Gamma_{15} \rightarrow \Gamma_1$ exciton, as proposed by Eisenberger *et al.*,¹¹ and peaks B and C which are situated at 13.1 and 15.3 eV are attributed to the $X'_2 \rightarrow X_3$ and $X'_5 \rightarrow X_3$ excitons. The more extended energy range of these peaks in CdF_2 than in CaF_2 (7.6 to 15.3 eV in CdF_2 ; 11.2 to 15.5 eV in CaF_2) is explained by the higher position of the d -level X_3 in the CdF_2 band scheme because of the repulsion by the cationic occupied $3d$ and $4d$ states. The greater energy separation between peaks B and C in CdF_2 (1.6 eV) than in CaF_2 (1.1 eV) is attributed to the wider valence band in CdF_2 . However, as was the case for CaF_2 , such an interpretation requires a lowering of the d^* bands in the band structure. Using the same method as before we obtain the energy scheme sketched in Fig. 9 with a well depth $A = -1.3$ Ry. The resulting energies of the d -like levels at Γ , X , and L can be found in Table V.

The next large peak which occurs in the CdF_2 reflection spectrum is situated at 23 eV. As for CaF_2 we have attributed it to the $\Gamma_{25}(p^-) \rightarrow \Gamma_{15}$ transition from the second set of valence bands (theoretical value 23.2 eV). Transitions from the occupied cationic d^* levels begin in our scheme at 25.4 eV [$\Gamma'_{25}(d^*) \rightarrow \Gamma_{15}$ and $\Gamma_{12}(d^*) \rightarrow \Gamma_{15}$]. These can explain the broad structures at about 27 and 30 eV which were absent in the CaF_2 spectrum. The slight difference between theoretical and experimental results is probably due to the neglect of the spin-orbit interaction (about 0.7 eV in the free Cd^{2+} ion⁵¹) in our calculation. The higher weak structures in the spectrum at about 38 eV has to be attributed, as for CaF_2 , to transitions from the $2s$ F^- states. More details on the comparison between the experimental data and our interpretation of the CaF_2 and CdF_2 spectra will be found in Table VI where the analogy between these two materials is clearly displayed.

IV. CONCLUSION

In this work, we have calculated the energy-band structure of both CaF_2 and CdF_2 with the same combined tight-binding pseudopotential method, with a semiempirical correction when dealing with the d excited states. From this study, several important points can be derived: (i) It has been shown that the cationic $4d^*$ levels did not perturb significantly the upper valence bands of CdF_2 which

are thus quite similar in shape to those of CaF_2 . (ii) The occurrence of the maximum of the valence band at the X point has been shown not to be unrealistic. On the other hand, the minimum of the conduction band is surely located at Γ in the two crystals. (iii) The similar shape of the low-energy peaks in the two reflection spectra can be explained by the great similarity between the upper valence bands and has led us to give the same assignment for these structures. (iv) Finally our band-structure calculations have been shown to be able to give a coherent interpretation of the two CaF_2 and CdF_2 experimental data.

APPENDIX

Universal valence bands for fluorite-type compounds

The limited tight-binding basis set is formed by the three orthogonal p anion orbitals. The resulting Hamiltonian matrix is 6×6 . Let V_σ and V_r denote the usual two center integrals between the first-neighbor anions and p_0 , the energy of the atomic anion p level in the crystal. With this first-neighbor approximation, the energies along symmetry axes Λ , Δ , and Σ are then given by:

$$\begin{aligned} \Delta_1 &: p_0 + 4V_r + 2V_\sigma \cos \eta\pi, \\ \Delta'_2 &: p_0 - 4V_r - 2V_\sigma \cos \eta\pi, \\ \Delta_3 &: p_0 \pm 2V_r (1 + \cos \eta\pi) \pm 2V_\sigma, \\ \Lambda_1 &: p_0 \pm 2(V_\sigma + 2V_r) \cos \frac{1}{2} \eta\pi, \\ \Lambda_3 &: p_0 \pm 2(V_\sigma + 2V_r) \cos \frac{1}{2} \eta\pi, \\ \Sigma_1 &: \begin{cases} p_0 + 2V_r(1 + \cos \frac{3}{4} \eta\pi) + 2V_\sigma \cos \frac{3}{4} \eta\pi, \\ p_0 - 4V_r \cos \frac{3}{4} \eta\pi - 2V_\sigma, \end{cases} \\ \Sigma_2 &: p_0 - 2V_r(1 + \cos \frac{3}{4} \eta\pi) - 2V_\sigma \cos \frac{3}{4} \eta\pi, \\ \Sigma_4 &: p_0 + 2V_r(1 + \cos \frac{3}{4} \eta\pi) + 2V_\sigma \cos \frac{3}{4} \eta\pi, \\ \Sigma_3 &: \begin{cases} p_0 - 2V_r(1 + \cos \frac{3}{4} \eta\pi) - 2V_\sigma \cos \frac{3}{4} \eta\pi, \\ p_0 + 4V_r \cos \frac{3}{4} \eta\pi + 2V_\sigma, \end{cases} \end{aligned}$$

where $0 < \eta < 1$ in all cases.

Taking $V_r/V_\sigma = -\beta$ ($\beta > 0$), one obtains at Γ , X , and L the following energies:

$$\begin{aligned} \Gamma_{15} &: p_0 + 2V_\sigma(1 - 2\beta), & \Gamma'_{25} &: p_0 - 2V_\sigma(1 - 2\beta), \\ X_1 &: p_0 - 2V_\sigma(1 + 2\beta), & X'_2 &: p_0 + 2V_\sigma(1 + 2\beta), \\ X_5 &: p_0 + 2V_\sigma, & X'_5 &: p_0 - 2V_\sigma, \\ L_1, L'_2, L_3, L'_3 &: p_0. \end{aligned}$$

The bands plotted in Fig. 5 are obtained with the same value of β as that of Pantelides, e.g., $\beta = \frac{1}{8}$ which gives a bandwidth of $5V_\sigma$ instead of $7.5V_\sigma$ as in the rocksalt structure. The resulting density of states has been calculated by the method of Gilat and Raubenheimer.⁵²

- ¹T. Tomiki and T. Miyata, *J. Phys. Soc. Jpn.* **27**, 658 (1969).
- ²G. Stephan, Y. le Calvez, J. C. Lemonier, and S. Robin, *J. Phys. Chem. Solids* **30**, 601 (1969).
- ³G. W. Rubloff, *Phys. Rev. B* **5**, 662 (1971).
- ⁴W. Hayes, A. B. Kunz, and E. E. Koch, *J. Phys. C* **50**, 200 (1971).
- ⁵A. le Comte and S. Robin, *Opt. Acta* **19**, 203 (1972).
- ⁶J. Frandon, B. Lahaye, and F. Pradal, *Phys. Status Solidi B* **53**, 565 (1972).
- ⁷B. Lahaye, thesis (Toulouse, 1973) (unpublished).
- ⁸R. T. Poole, J. Szajman, R. C. G. Leckey, J. C. Jenkins, and J. Liesegang, *Phys. Rev. B* **12**, 5872 (1975).
- ⁹W. Bremser (unpublished) cited in H. Wiesner and B. Hönerlage, *Z. Phys.* **256**, 43 (1972).
- ¹⁰R. A. Forman, W. R. Hosler, and R. F. Blunt, *Solid State Commun.* **10**, 19 (1972).
- ¹¹P. Eisenberger and M. G. Alderstein, *Phys. Rev. B* **1**, 1787 (1970).
- ¹²J. M. Berger, G. Leveque, and J. Robin, *C. R. Acad. Sci. (Paris)* **279**, 512 (1974).
- ¹³A. J. Bourdillon and J. H. Beaumont, *J. Phys. C* **9**, L473 (1976).
- ¹⁴N. V. Starostin and V. A. Ganin, *Fiz. Tverd. Tela* **15**, 3404 (1973) [*Sov. Phys.-Solid State* **15**, 2265 (1974)].
- ¹⁵N. V. Starostin and M. P. Shepilov, *Fiz. Tverd. Tela* **17**, 822 (1975) [*Sov. Phys.-Solid State* **17**, 523 (1975)].
- ¹⁶V. A. Ganin, M. G. Karin, V. K. Sidorin, K. K. Sidorin, N. V. Starostin, G. P. Startsev, and M. P. Shepilov, *Fiz. Tverd. Tela* **16**, 3554 (1974) [*Sov. Phys.-Solid State* **16**, 2313 (1975)].
- ¹⁷N. V. Starostin, *Fiz. Tverd. Tela* **11**, 1624 (1969) [*Sov. Phys.-Solid State* **11**, 1317 (1969)].
- ¹⁸N. Daude, C. Jouanin, and C. Gout, *Phys. Rev. B* **15**, 2399 (1977).
- ¹⁹U. Seth and R. Chaney, *Phys. Rev. B* **12**, 5923 (1975).
- ²⁰L. F. Mattheiss, *Phys. Rev. B* **5**, 290 (1972).
- ²¹S. Tewari, *Solid State Commun.* **12**, 437 (1973).
- ²²K. Maschke and U. Rossler, *Phys. Status Solidi* **28**, 577 (1968).
- ²³A. Breeze and P. G. Perkins, *Solid State Commun.* **13**, 1031 (1973).
- ²⁴T. H. Lee and F. Moser, *Phys. Rev. B* **3**, 347 (1971).
- ²⁵F. Bassani, R. S. Knox, and W. B. Fowler, *Phys. Rev.* **137**, A1217 (1965).
- ²⁶J. P. Albert, C. Jouanin, and C. Gout, *Phys. Rev. B* (to be published); J. P. Albert, thesis (Montpellier, 1975) (unpublished).
- ²⁷J. P. Albert, C. Jouanin, and C. Gout, *Solid State Commun.* **22**, 199 (1977).
- ²⁸C. Jouanin, J. P. Albert, and C. Gout, *Nuovo Cimento B* **28**, 483 (1975).
- ²⁹C. Jouanin, J. P. Albert, and C. Gout, *J. Phys.* **37**, 595 (1976).
- ³⁰J. W. Richardson, M. J. Blackman, and J. E. Rano-chak, *J. Chem. Phys.* **58**, 3010 (1973).
- ³¹C. Salez (private communication).
- ³²J. C. Slater, *Phys. Rev.* **81**, 385 (1951).
- ³³F. Bassani and E. S. Giulano, *Nuovo Cimento B* **8**, 193 (1972).
- ³⁴E. S. Giulano and R. Ruggeri, *Nuovo Cimento B* **6**, 53 (1969).
- ³⁵J. C. Philipps and L. Kleinman, *Phys. Rev.* **116**, 287 (1959).
- ³⁶N. Daude, C. Gout, and C. Jouanin, *Phys. Rev. B* **15**, 3229 (1977).
- ³⁷S. T. Pantelides, *Phys. Rev. B* **11**, 5082 (1975).
- ³⁸W. B. Fowler, *Phys. Rev.* **151**, 657 (1966).
- ³⁹F. Perrot, *Phys. Status Solidi* **52**, 163 (1972).
- ⁴⁰S. T. Pantelides, D. J. Mickish, and A. B. Kunz, *Phys. Rev. B* **10**, 2602 (1974).
- ⁴¹N. F. Mott and M. J. Littleton, *Trans. Faraday Soc.* **34**, 485 (1938).
- ⁴²B. Vasvari, A. O. Animalu, and V. Heine, *Phys. Rev.* **154**, 535 (1967).
- ⁴³J. W. McCaffrey, J. R. Anderson and D. A. Papaconstantopoulos, *Phys. Rev. B* **7**, 674 (1973).
- ⁴⁴C. Lopez Rios and C. B. Sommers, *Phys. Rev. B* **6**, 2181 (1975).
- ⁴⁵R. C. Whited and W. C. Walker, *Phys. Rev.* **188**, 1380 (1969).
- ⁴⁶See, for example, R. A. Deegan, and W. D. Twose, *Phys. Rev.* **164**, 993 (1967); J. A. Moriarty, *Phys. Rev. B* **6**, 4445 (1972); R. A. Deegan, *Phys. Rev.* **188**, 1170 (1969), and papers cited therein.
- ⁴⁷C. Y. Fong and M. L. Cohen, *Phys. Rev. Lett.* **24**, 306 (1970).
- ⁴⁸A. O. E. Animalu, *Phys. Rev. B* **8**, 3542 (1973).
- ⁴⁹C. Y. Fong and M. L. Cohen, *Phys. Rev.* **185**, 1168 (1969).
- ⁵⁰B. Hönerlage and H. Wiesner, *Z. Phys.* **242**, 406 (1971).
- ⁵¹F. Herman and S. Skillman, *Atomic Structure Calculations* (Prentice-Hall, Englewood Cliffs, N.J., 1963), pp. 2-9.
- ⁵²G. Gilat and L. J. Raubenheimer, *Phys. Rev.* **144**, 390 (1966).